Electronic structure, magnetic properties, and Mössbauer isomer shifts of Fe and Ti*Fe* alloys

Diana Guenzburger
Argonne National Laboratory, 9700 South Cass Avenue, Argonne, Illinois 60439
and Department of Physics and Astronomy, Northwestern University, Evanston, Illinois 60201

D. E. Ellis
Department of Physics and Astronomy, Northwestern University, Evanston, Illinois 60201
(Received 4 May 1984)

The self-consistent discrete variational method and the local $X\alpha$ exchange approximation have been employed to obtain the electronic structure of 15-atom clusters representing Fe metal and Ti*Fe* alloys. The dependence of the magnetic moment and isomer shift of iron metal on pressure was investigated. Local moments of Ti dilute impurities in Fe were calculated. The ordered (CsCl-structure) intermetallic compound FeTi, which represents a concentrated-impurity limit of the Ti*Fe* alloys, was also studied, and an isomer-shift (IS) value obtained. The results show that the cluster approach yields magnetic moments and IS consistent with experimental magnetization, neutron scattering, and Mössbauer data.

I. INTRODUCTION

The problem of dilute alloys of transition elements in a ferromagnetic host has been of long-standing interest. Apart from the standard semiempirical approaches,[1] band-structure calculations would provide many answers to the local or itinerant properties observed by the experimentalists. However, in the case of dilute alloys or structural disorder, first-principles band calculations, even with the now available powerful computers, would be very cumbersome because of the large number of atoms to be included in the unit cell.

An approach which avoids this difficulty, although still retaining the first-principles aspect of the calculations, is to study the electronic structure of clusters representing the alloys. This approach has been applied to a significant number of cases,[2–4] and the results obtained encourage further applications.

We have undertaken an investigation of the electronic structure of Fe metal, and Fe containing Ti in dilute concentrations. The choice of such systems was based on the following considerations: First, Fe and Ti are transition elements, with Fe on the $3d$-electron-rich side, compared to Ti. Observing the Pauling electronegativities (1.8 for Fe, 1.5 for Ti), one may expect that charge transfer will take place among the atoms, and a more quantitative estimate of this effect would be desirable. The alloying of a ferromagnetic host with a nonmagnetic metal raises interesting questions about which conditions favor or suppress the existence of local moments. Some experimental data are available regarding local moments,[5] against which our results may be checked; in some other cases, we make predictions and hope that future experimental data will allow an assessment of our results. Many measurements on hyperfine interactions have been made on such systems with Mössbauer spectroscopy of ^{57}Fe.[6,7] We report here calculations of isomer shifts, and interpret the values found in terms of the electronic structure.

In addition to treating clusters representing Fe and dilute alloys of Ti in the Fe host, we have also investigated the inverse case, in which Fe is an impurity or a dilute solute in the nonmagnetic metals Ti and Zr. The results for these alloys, which have quite different characteristics, will be presented in a subsequent paper.

II. THEORETICAL APPROACH

A. Electronic structure

In Fig. 1 we show the 15-atom cluster which is chosen to represent the alloys. Only the bcc structure was considered.

The electronic structure of the cluster was obtained with use of the first-principles discrete variational method (DVM), and the local $X\alpha$ approximation for the exchange interaction. Since the method has been described in detail in many publications,[8,9] we only give here an outline of its main features. The DVM, as implemented within the framework of a molecular-orbital method, has numerous successful applications, including the study of magnetic

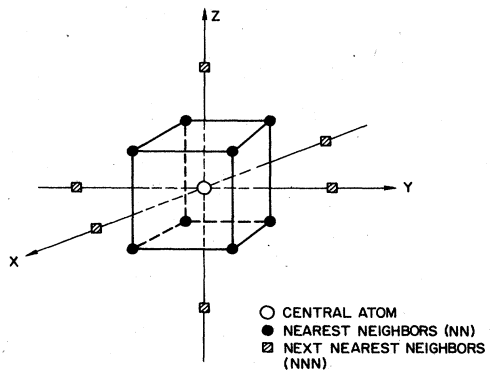

FIG. 1. 15-atom cluster representing bcc metals or alloys.

impurities in Ag and Pd,[4] and other properties of metals and alloys treated as clusters.[10]

The one-electron Hamiltonian for the cluster is a functional of the electronic density

$$h_\sigma = -\tfrac{1}{2}\nabla^2 + V_{\text{Coul}}(\rho) + V_{X\alpha}(\rho_\sigma) \tag{1}$$

in Hartree atomic units, where the electronic density at some point $\vec{r}$ is a sum over the molecular spin orbitals ϕ_{j_σ} with occupation n_{j_σ}:

$$\rho_\sigma(\vec{r}) = \sum_j n_{j_\sigma} |\phi_{j_\sigma}(\vec{r})|^2 . \tag{2}$$

The Coulomb potential has an electronic and a nuclear part:

$$V_{\text{Coul}}(\rho) = \int \frac{\rho(\vec{r}\,')d\vec{r}\,'}{|\vec{r}-\vec{r}\,'|} - \sum_k \frac{Z_k}{|\vec{r}-\vec{R}_k|} , \tag{3}$$

where Z_k is the atomic number of nucleus k at distance $\vec{R}_k$ from the electron, and $\rho = \rho_\uparrow + \rho_\downarrow$ is the total charge density. The exchange potential is a function of the spin density:

$$V_{X\alpha}(\rho_\sigma) = -3\alpha \left[\frac{3\rho_\sigma(\vec{r})}{4\pi} \right]^{1/3} , \tag{4}$$

and the value $\alpha = \frac{2}{3}$ was adopted here, since it is the value which is variationally compatible with the one-electron equations:[9]

$$(h_\sigma - \epsilon_{i\sigma})\phi_{i\sigma}(\vec{r}) = 0 . \tag{5}$$

Allowing the spatial part of the spin orbitals $\phi_{i\sigma}$ to be different for different spins will lead to spin polarization, in addition to the contributions of unpaired spins.

The molecular orbitals are expanded on a basis of atomic numerical orbitals (LCAO approximation). Spherical potential wells around the atoms are used to obtain more contracted valence orbitals for the basis, which includes the $3d$, $4s$, and $4p$ orbitals for both Ti and Fe. The secular equations

$$(\underline{H} - \underline{E}\underline{S})\underline{C} = \underline{0} \tag{6}$$

are finally solved self-consistently, using matrix elements determined by numerical integration.

The three-dimensional integrations of the DVM method are usually performed on a random-points grid by the diophantine method.[8] However, for this special case of calculations of hyperfine interactions of rather large atoms, which have important contributions from core electrons that have to be taken into account to get meaningful results, a special integration scheme was used in the region around the nucleus of the atom considered as the Mössbauer probe. This is necessary to get better wave functions in the core region of rapid variation. A sphere of radius ~ 2 a.u. is considered around the probe nucleus, and a systematic polynomial integration[11] in three dimensions is performed.

Finally, an embedding scheme is used to simulate the metal outside the cluster. This has been described elsewhere,[10] and basically consists of placing atomic potentials on a number of sites around the cluster. These potentials are truncated to simulate orthogonality effects.

B. Mössbauer isomer shifts

We have made calculations of the isomer shifts (IS) for these alloys. Since these interactions constitute very small effects special care must be taken regarding the numerical procedures. The IS is defined as[12]

$$\delta_{\text{IS}} = \frac{2\pi}{3} Ze^2 (\Delta\langle r^2\rangle) S'(Z)[\rho_A(0) - \rho_S(0)] \tag{7}$$

or, equivalently:

$$\delta_{\text{IS}} = \alpha[\rho_A(0) - \rho_S(0)] . \tag{8}$$

α in Eq. (8) includes the terms in Eq. (7) which refer to the Mössbauer nucleus. Z is the nuclear charge, $\Delta\langle r^2\rangle$ the difference in the mean-square nuclear radius between excited and ground states of the nuclear transition involved, $\rho(0)$ is the total charge density at the probe nucleus, and the parameter $S'(Z)$ accounts for relativistic effects. In Eq. (7), A and S refer to absorber and source. In principle, all orbitals of s-type symmetry have nonvanishing contributions to the density at the nuclear site; however, in our calculations we have excluded the contributions from the deep core $1s$ and $2s$ orbitals of Fe, since our numerical precision is still not good enough to give significant values for them, as they represent very small differences between very large numbers. Fortunately, atomic calculations for Fe in different oxidation states show that differences in the electronic density at the origin for the $1s$ and $2s$ orbitals are quite negligible.[13]

III. RESULTS AND DISCUSSION

A. Properties of the Fe host

The much studied case of the electronic structure of Fe metal is an ideal example to test our cluster model, besides being our host metal, to which the properties of the alloys should be compared. Several Fe-metal band-structure calculations are reported,[14,15] as well as a cluster calculation with the multiple-scattering $X\alpha$ (MS $X\alpha$) method.[2]

We have obtained the electronic structure for the Fe_{15} embedded cluster in both an all-electron scheme and one in which the deep core orbitals $1s$, $2s$, and $2p$ are kept "frozen" and orthogonal to the molecular orbitals. The results of this last procedure do not differ in any significant manner from the all-electron procedure, including the evaluation of the IS, and so this computationally less expensive "frozen-core" scheme was adopted for most of the clusters calculated.

In Fig. 2 the total density of states for the valence and conduction bands of Fe metal is shown. Since in the cluster model we obtain a discrete set of energy levels, these are "broadened" by Lorentzian functions to simulate a continuum. The spin ↑ and spin ↓ bands in this and other density of states diagrams are normalized to a fixed peak height, and *not* to the total number of electrons. One can see clearly the ferromagnetic nature of the metal appearing, as in the Stoner model. However, the density of states does not compare very well with recent band-

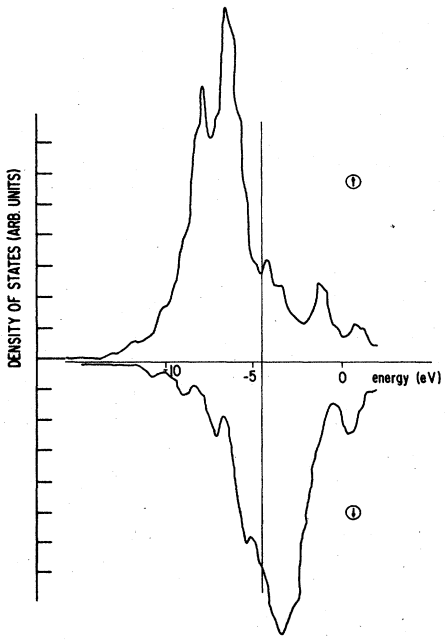

FIG. 2. Total density of states for the Fe_{15} cluster in a spin-polarized calculation, including $3d$, $4s$, and $4p$ contributions.

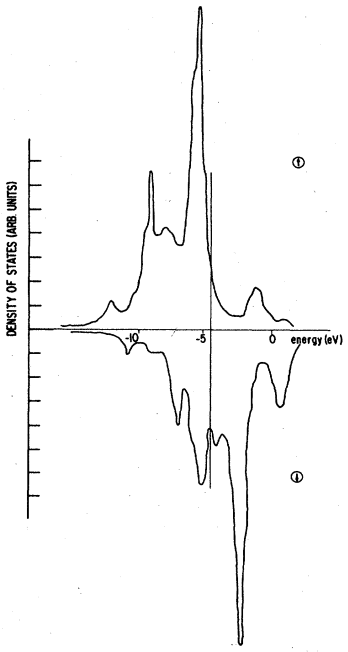

FIG. 3. Local density of states at the central Fe atom in the Fe_{15} cluster.

structure calculations,[14,15] and does not show much structure.

A much better diagram, as compared to band calculations, is obtained by considering only the *local* density of states on the central Fe atom. This is shown in Fig. 3, which shows quite good agreement with the density of states obtained by Moruzzi, Janak, and Williams,[15] considering the size of our cluster. Indeed, intuition would indicate that the central atom, due to its environment in the cluster being more similar to that of a metallic atom, will be the one showing the most bulklike properties. As one goes outwards in the cluster, we arrive at the last shell, whose atoms should be expected to show a surfacelike behavior, between bulk atoms and free atoms. All our results confirm this conclusion, as shall be seen as we proceed further, so we have chosen in all cases the central atom for the evaluation of local properties. We point out, however, that investigators who apply the MS $X\alpha$ method to isolated metal clusters do not share this point of view; rather, they seem to conclude that the outer atoms of the cluster are the most bulklike.[2]

Several factors which have a bearing on this discrepancy can be mentioned:

(1) The boundary conditions used in MS and DV calculations are different. The MS method uses isolated cluster boundary conditions with decaying Coulomb wave solutions in the exterior region. The DV method makes an expansion in atom-centered orbitals, with the cluster embedded in the potential field of the infinite solid. We have verified that the embedding field has a significant effect on the central atom, density of states (DOS), charge, and spin densities. This effect is *indirect,* in that "surface" atoms are most affected by the crystalline hosts, and their interaction with the central atom is thereby modified.

(2) The potentials used in MS and DV calculations are different. The MS method uses a truncated muffin-tin approximation to the potential, while the DV method expands the potential in a set of basis functions, with amplitudes determined either from Mulliken atomic orbital populations (self-consistent charge approximation) or by least-square procedures (self-consistent multipolar approximation). It is possible that differences in the potential in the interstitial region, which is treated as a constant in the MS approach, affect the s-d hybridization sufficiently to modify the central atom DOS. This effect must become negligible in the limit of large clusters, as seen by comparison of various band-structure approaches.

(3) Finally, there are reasons to be cautious about focusing attention entirely on the central site in a highly symmetric cluster. For example, in cubic clusters with O_h symmetry, the central d orbitals contribute only to t_{2g} and e_g representations, while d orbitals of the first coordination shell contribute to a variety of symmetries. We thus can understand that the central-site DOS may converge slowly to the bulk limit with increasing cluster size.

In Table (I) we present some relevant results for the Fe_{15} cluster. The equilibrium lattice parameter was considered, and calculations were also performed for compressed interatomic distances, since experimental data is available both for the magnetic moments and the IS for Fe under pressure. The variation of the lattice parameter with pressure has been reported,[16] and the variation of the magnetic moment with pressure observed experimentally follows the relation:[15]

$$\frac{\partial \ln M}{\partial P} = -0.32 \text{ Mbar}^{-1} . \tag{9}$$

The IS values were derived by combining Eq. (8) with the experimental relation obtained by Williamson,

TABLE I. Magnetic moments and isomer shifts of the embedded Fe_{15} cluster.

Lattice parameter (Å)	Pressure[a] (kbar)	μ[b] (expt.) (μ_B)	μ calculated (μ_B) Fe_C	Fe_{NN}	Fe_{NNN}	IS[c] (expt.) (mm/s)	IS[d] (calc.) (mm/s)
2.866	0	2.17	2.80	3.39	3.67	0	0
2.825	80	2.12	2.78	3.32	3.60	−0.058	−0.055
2.805	122	2.09	2.77	3.30	3.57	−0.086	−0.086
2.764	250	2.00	2.73	3.29	3.58	−0.145	−0.145
2.658	781	1.69	2.57	3.22	3.54	−0.300	−0.340

[a]From Ref. 16.
[b]$\partial \ln M/\partial P$ ($Mbar^{-1}$) $= -0.32$ (see Ref. 15).
[c]From Ref. 6.
[d]$\rho(0)$ calculated for the central Fe atom.

Bukshpan, and Ingalls[6]

$$\frac{\alpha \partial \rho(0)}{\partial \ln V} = 1.33 \text{ (at 300 K)} . \tag{10}$$

Both calculated and experimental values are shifts relative to Fe metal.

For pressures greater than ~130 kbar, bcc Fe undergoes a structural phase transition to hcp Fe. The dotted line in Table I separates the calculations for which the experimental data is actually available, from the higher pressures, for which "experimental" moments and IS values have been derived with the same empirical relations, but actual measurements are still to be obtained in the future, if some technique is found which will stabilize the bcc phase at higher pressures.

Observing the moments obtained for the cluster, which were calculated by taking the difference between the Mulliken populations[17] for spin ↑ and spin ↓ electrons ($3d$, $4s$, and $4p$), three points may be mentioned:

(a) The local magnetic moments on the central Fe, and on the first and second shell of neighbors, are higher than the experimental value, at atmospheric and higher pressures. This shows that, although the moments are lower than the atomic value, the cluster is not yet large enough to describe the collective effect in the bulk which reduces the Fe moments to $2.2\mu_B$.

(b) The central Fe atom has the lowest calculated value of the moment, and thus the closest to experiment. The moments increase outwards. This is another indication, as with the local density of states, that it is the central atom which is best described as a bulk atom.

(c) The trend of the moment with pressure is reproduced in the calculations; however, the calculated decrease of the moment with pressure is less pronounced than what is found experimentally.

Although the experimental values for pressures higher than 130 kbar are extrapolations, recent band-structure calculations by Bagayoko and Callaway[18] give theoretical values at lattice parameters corresponding to 250 and 781 kbars which are very close to the empirical values. This suggests that the magnetic behavior at higher pressures would follow the same law, if the bcc structure was preserved.

The IS values were obtained with the nuclear parameter $\alpha = -0.25$ (mm a_0^3/sec), which fits best the lower pressure values and is very close to the best theoretical estimates.[19,20] The agreement with experiment is excellent for the lower pressures, and since a similar agreement is found for the high-pressure predictions, this suggests that the empirical law in Eq. (10) would still be followed in this case.

The decrease of the IS with pressure is due almost entirely to an increase in the valence ($4s$-type) electronic density at the nucleus. This is because of the fact that the probe atom's valence orbitals of a_1 symmetry have to be orthogonal to the core orbitals of the neighbors, causing a contraction of the wave functions towards the nucleus, which increases with decreasing lattice parameter.

B. Ti impurity in Fe

The case of a very dilute Ti impurity in bcc Fe was studied by substituting the central atom of the cluster in Fig. 1 by Ti, while keeping all the other Fe atoms. We have first made a self-consistent calculation for the Fe lattice parameter (2.866 Å). Figure 4 depicts the local density of states on the Ti atom. The diagram shows the negative moment that builds up on the Ti, antiferromagnetically coupled to the Fe lattice moments.

Table II gives the calculated local moments for this

TABLE II. Magnetic moments of Ti impurities in Fe.

Cluster[a]	Lattice parameter (Å)	μ[b] (expt.) (μ_B)	μ calculated (μ_B) Ti	Fe_{NN}	Fe_{NNN}
$TiFe_8Fe_6$	2.866	−2.28	−2.18	3.28	3.66
$TiFe_8Fe_6$	3.06		−2.61	3.68	3.99
$Ti(TiFe_7)Fe_6$	2.866		−2.04	3.34	3.72

[a]All clusters are embedded in the Fe metal.
[b]From Ref. 5. Experimental value given here includes the diffuse component, quoted by the authors in Ref. 5 as $-0.2\mu_B$.

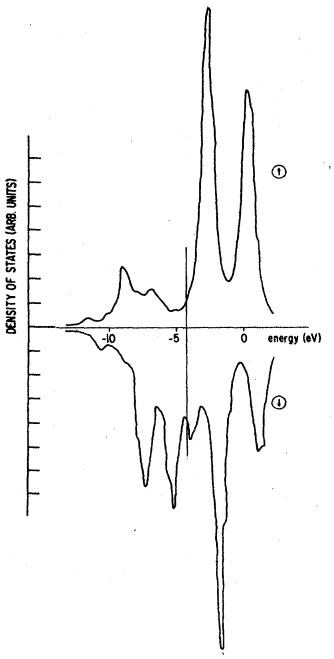

FIG. 4. Local density of states at the central Ti atom in the $TiFe_{14}$ cluster, embedded in the Fe metal.

case. Recently, neutron scattering experiments were reported by Kajzar and Parette[5] for very low concentrations of Ti in Fe. For the lowest concentration measured (0.84 at. %), a moment of $-2.28\mu_B$ is found, in good agreement with our calculated value.

Kajzar and Parette also report values for slightly higher concentrations of the impurity, and a very large *decrease* of the moment on the Ti is observed, while the moment on the Fe is considerably more stable. To investigate some possible causes for such behavior, we have made two more self-consistent calculations, for which the results are also seen in Table II. A local expansion of the lattice would produce a larger moment on Ti, probably because the driving moments on the surrounding Fe atoms tend to higher values. However, the actual average interatomic distances *increase* slightly at *higher* concentrations,[5] so obviously a local expansion would produce an inverse effect to that actually observed.

The third calculation reported in Table II aims at investigating the possibility of clustering of the Ti atoms, as a cause for the dependence of the moment on concentration. In this case, a nearest-neighbor Fe atom was substituted for a Ti atom, creating a Ti-Ti pair in the Fe host. The symmetry in this case is lowered to C_{3v}. The moment calculated on Ti is smaller than on the isolated impurity, suggesting that clustering may be the cause for the decrease of the antiferromagnetically coupled moment of Ti in Fe, at higher Ti concentrations.

We mention that coherent potential approximation (CPA) calculations failed to describe the magnetic moments at very dilute concentrations,[5] while describing the more concentrated alloys relatively well. However, an earlier model using the virtual bound state concept produced a value of $-2\mu_B$ on Ti in the dilute limit.[21]

C. The compound FeTi

We end our report by giving some results relative to the 50%-50% compound FeTi, which represents the concentrated limit of TiFe alloys. It seems now well established[22] that the lattice has the CsCl structure, that is, no Ti has a Fe first neighbor, and vice versa, no Fe has a Ti neighbor. Our cluster in Fig. 1 can represent this case in two ways, the first with Fe in the center, Ti atoms at the nearest-neighbor (NN) shell, Fe atoms as next-nearest neighbors, and finally, the whole cluster embedded in a Ti environment. The second case depicts the inverse situation, that is, Ti is the central atom, Fe are nearest neighbors etc. The goal of this second self-consistent calculation was to verify if spurious cluster-size effects were artificially altering the results by any significant amount.

Table III shows results for the FeTi compound. We definitely find a sizable moment on the Ti atoms, coupled antiferromagnetically to Fe (see also the density-of-states diagram in Fig. 5). This result repeats itself for the second cluster, where the order of the Fe and Ti atoms is reversed. We are not aware of neutron scattering measurements of the spin distribution in these compounds; a Mössbauer spectroscopy study reported showed no sign of a magnetic moment on the Fe.[23] Magnetic susceptibility measurements for TiFe do not clarify the issue of magnetic ordering.[24] If indeed TiFe is a Pauli paramagnet, then the magnetic moments found for our clusters may be ra-

TABLE III. Magnetic moments and isomer shifts of the (CsCl-structure) FeTi intermetallic compound.

Cluster	Lattice parameter (Å)	μ calculated (in μ_B) central atom	NN atom	NNN atom	$\rho(0)$ (a_0^{-3})	IS (calc.) (mm/s)	IS[b] (expt.) (mm/s)
Fe_{15}	2.866	2.80	3.39	3.67	3s 139.93 valence 6.53 146.46	0	0
$FeTi_8Fe_6$	2.95[a]	2.09	−1.58	4.06	3s 140.01 valence 7.04 147.05	−0.148	−0.145
$TiFe_8Ti_6$	2.95	−1.65	3.46	−2.02			

[a]From Ref. 25.
[b]From Ref. 7.

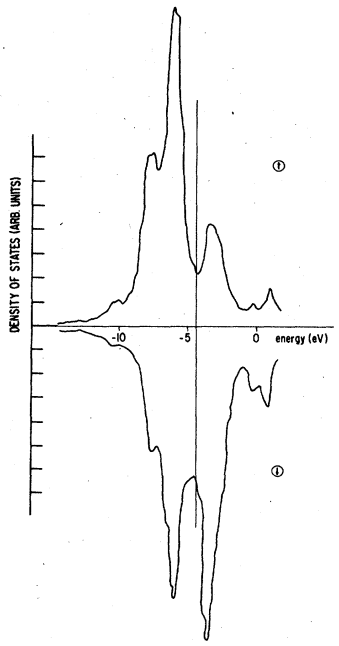

FIG. 5. Local density of states at the central Fe atom for the intermetallic compound FeTi, represented by the cluster $FeTi_8Fe_6$ embedded in Ti metal.

tionalized as a cluster-size effect. The calculated next-nearest-neighbor (NNN) moments (see Table III) are similar to those of free atoms, consistent with their position as "surface atoms." These atoms in turn induce sizable moments on nearest neighbors and the central site. The present potential-embedding scheme is apparently not capable of reproducing adequately the *magnetic* coupling between host and cluster. The most straightforward test of these ideas would be to increase the cluster size by addition of another coordination shell; this is, however, beyond the scope of the present work.

In Table III we also give the IS value of FeTi, relative to Fe metal, and compare it to the experimental value. We use here the same value of the nuclear constant α ($=-0.25$) that was employed for Fe at different pressures. We verify that also in this case the agreement is excellent. The charge transferred from the Ti neighbors into the central Fe atom is 0.31 electrons. Also given in the table are the values of $\rho(0)$ for Fe and FeTi, at the central Fe nucleus of the cluster. We can easily relate the IS value mainly to the Ti→Fe charge transfer, which builds up the valence electronic density at the nucleus in FeTi.

IV. CONCLUSIONS

We have performed self-consistent electronic structure calculations for clusters representing the Fe metal and Ti*Fe* alloys, in order to study mainly magnetic moments and isomer shifts. We find that our cluster model gives excellent agreement with experiment regarding the dependence of the IS with pressure in Fe metal. This agreement is also found for the intermetallic compound FeTi. As far as magnetic moments are concerned, overall qualitative agreement is found for Fe under pressure, and excellent agreement is found for the case of Ti*Fe* in the dilute limit. The local moments found in the calculations for the FeTi compound are not confirmed by Mössbauer experiments reported; perhaps future work with neutron scattering will help clarify this point.

In conclusion, we believe that the calculations of localized properties in metals and alloys with a cluster model have come to a point where reliable information is derived, which cannot as yet be obtained by other first-principles methods. The results may be improved further by adding one or more shells of atoms to the cluster. This would represent a sizable increase in the computational effort; our results and other similar studies[2] have shown, however, that 15-atom clusters are already sufficiently large to account for many properties of the bulk metals, especially those that are localized.

ACKNOWLEDGMENTS

One of the authors (D.G.) is grateful for many interesting discussions with E. Galvão da Silva, who suggested the problem. This work was supported in part by the U. S. Department of Energy, the U. S. National Science Foundation, Grant No. INT-83-12863 and by Conselho Nacional de Desenvolvimento Científico e Tecnológico (CNPq) of Brazil.

[1]J. Friedel, Nuovo Cimento Suppl. 7, 287 (1958); P. W. Anderson, Phys. Rev. 124, 41 (1961); P. A. Wolff, *ibid.* 120, 814 (1960); 124, 1030 (1961).

[2]C. Y. Yang, K. H. Johnson, D. R. Salahub, J. Kaspar, and R. P. Messmer, Phys. Rev. B 24, 5673 (1981), and references therein.

[3]J. Kaspar and D. R. Salahub, J. Phys. F 13, 311 (1983), and references therein.

[4]B. Delley, D. E. Ellis, and A. J. Freeman, J. Magn. Magn. Mater. 30, 71 (1982).

[5]F. Kajzar and G. Parette, Phys. Rev. 20, 2002 (1979).

[6]D. L. Williamson, S. Bukshpan, and R. Ingalls, Phys. Rev. B 6, 4194 (1972).

[7]E. V. Mielczarek and W. P. Winfree, Phys. Rev. B 11, 1026 (1975).

[8]D. E. Ellis, Int. J. Quantum. Chem. S2, 35 (1968); D. E. Ellis, and G. S. Painter, Phys. Rev. B 2, 2887 (1970); A. Rosén, D. E. Ellis, H. Adachi, and F. W. Averill, J. Chem. Phys. 85, 3629 (1976).

[9]J. C. Slater, *The Self-consistent Field for Molecules and Solids,* Vol. 4 of Quantum theory of Molecules and Solids (McGraw-Hill, New York, 1974).

[10]G. A. Benesh and D. E. Ellis, Phys. Rev. B 24, 1603 (1981).

[11]A. H. Stroud, *Approximate Calculation of Multiple Integrals,* (Prentice-Hall, Englewood Cliffs, N.J., 1971).

[12]See, for example, N. N. Greenwood and T. C. Gibb, *Mössbauer Spectroscopy* (Chapman and Hall, London, 1971); J. M. Friedt and J. Danon, in *Modern Physics in Chemistry*

edited by E. Fluck and V. I. Goldanskii (Academic, London, 1979), Vol. 2; B. D. Dunlap and G. M. Kalvius, in *Mössbauer Isomer Shifts,* edited by G. K. Shenoy and F. E. Wagner (North-Holland, Amsterdam, 1978).

[13]J. V. Mallow, A. J. Freeman, and J. P. Desclaux, Phys. Rev. B **13**, 1884 (1976).

[14]J. Callaway and C. S. Wang, Phys. Rev. B **16**, 2095 (1977).

[15]V. L. Moruzzi, J. F. Janak, and A. R. Williams, *Calculated Electronic Properties of Metals* (Pergamon, New York, 1978).

[16]H. Mao, W. A. Bassett, and T. Takahashi, J. Appl. Phys. **38**, 272 (1967).

[17]R. S. Mulliken, J. Chem. Phys. **23**, 1833 (1955).

[18]D. Bagayoko and J. Callaway, Phys. Rev. B **28**, 5419 (1983).

[19]D. Guenzburger, D. M. S. Esquivel, and J. Danon, Phys. Rev. **18**, 4561 (1978).

[20]W. C. Nieuwpoort, D. Post, and P. Th. Van Duijnen, Phys. Rev. B **17**, 91 (1978).

[21]I. A. Campbell and A. A. Gomes, Proc. Phys. Soc. London **91**, 319 (1967).

[22]N. Motta, M. De Crescenzi, and A. Balzarotti, Phys. Rev. B **27**, 4712 (1983).

[23]G. Rupp, Z. Phys. **230**, 265 (1970).

[24]M. V. Nevitt, J. Appl. Phys. **31**, 155 (1960).

[25]M. Hansen, *Constitution of Binary Alloys* (McGraw-Hill, New York, 1958).